THE JOURNAL OF BIOLOGICAL CHEMISTRY Vol. 277, No. 23, Issue of June 7, pp. 20833–20839, 2002
Printed in U.S.A.

Structure-based Design of β1,4-Galactosyltransferase I (β4Gal-T1) with Equally Efficient *N*-Acetylgalactosaminyltransferase Activity

POINT MUTATION BROADENS β4Gal-T1 DONOR SPECIFICITY*

Received for publication, November 21, 2001, and in revised form, March 18, 2002
Published, JBC Papers in Press, March 26, 2002, DOI 10.1074/jbc.M111183200

Boopathy Ramakrishnan‡§ and Pradman K. Qasba‡¶

From the ‡Structural Glycobiology Section and §Intramural Research Support Program-SAIC, Laboratory of Experimental and Computational Biology, Center for Cancer Research, NCI-Frederick, National Institutes of Health, Frederick, Maryland 21702

β1,4-Galactosyltransferase I (Gal-T1) normally transfers Gal from UDP-Gal to GlcNAc in the presence of Mn^{2+} ion. In the presence of α-lactalbumin (LA), the Gal acceptor specificity is altered from GlcNAc to Glc. Gal-T1 also transfers GalNAc from UDP-GalNAc to GlcNAc, but with only ~0.1% of Gal-T activity. To understand this low GalNAc-transferase activity, we have carried out the crystal structure analysis of the Gal-T1·LA complex with UDP-GalNAc at 2.1-Å resolution. The crystal structure reveals that the UDP-GalNAc binding to Gal-T1 is similar to the binding of UDP-Gal to Gal-T1, except for an additional hydrogen bond formed between the *N*-acetyl group of GalNAc moiety with the Tyr-289 side chain hydroxyl group. Elimination of this additional hydrogen bond by mutating Tyr-289 residue to Leu, Ile, or Asn enhances the GalNAc-transferase activity. Although all three mutants exhibit enhanced GalNAc-transferase activity, the mutant Y289L exhibits GalNAc-transferase activity that is nearly 100% of its Gal-T activity, even while completely retaining its Gal-T activity. The steady state kinetic analyses on the Leu-289 mutant indicate that the K_m for GlcNAc has increased compared to the wild type. On the other hand, the catalytic constant (k_{cat}) in the Gal-T reaction is comparable with the wild type, whereas it is 3–5-fold higher in the GalNAc-T reaction. Interestingly, in the presence of LA, these mutants also transfer GalNAc to Glc instead of to GlcNAc. The present study demonstrates that, in the Gal-T family, the Tyr-289/Phe-289 residue largely determines the sugar donor specificity.

β1,4-Galactosyltransferase I (β4Gal-T1,[1] EC 2.4.1.38) catalyzes the transfer of galactose (Gal) from UDP-Gal to the *N*-acetylglucosamine (GlcNAc) residue present at the nonreducing terminal end of glycans of glycoproteins and glycolipids (1), producing β1,4-linked galactosylated glycan. In addition to GlcNAc as an acceptor, the enzyme can also use other sugars, such as *N*-acyl-substituted glucosamines and *N*-acetyl-D-mannosamine, as acceptors (2). The enzyme does not have an absolute requirement for the sugar donor UDP-Gal; instead, it exhibits polymorphic donor specificity, in that it also transfers glucose (Glc), D-deoxy-Glc, arabinose, GalNAc, and GlcNAc from their UDP derivatives, albeit at low rates (0.3–5%) compared with Gal transfer (3–7).

α-Lactalbumin (LA), a mammary gland-specific calcium-binding protein, alters the sugar acceptor specificity of Gal-T1 toward Glc (8). This activity is described as the lactose synthase (LS) activity of β4Gal-T1 (EC 2.4.1.22). LA has been shown to alter not only the sugar acceptor specificity of the enzyme, but also its sugar donor specificity (7, 9), because it stimulates the transfer of Glc from UDP-Glc to GlcNAc. Similarly, it has been shown previously that the transfer of GalNAc from UDP-GalNAc to GlcNAc by Gal-T1 is also enhanced in the presence of LA (5). To better understand the modulation of substrate specificity, we had carried out a series of studies on the crystal structure of LA·Gal-T1 complex with various substrates (7, 10). Analysis of the molecular interactions between LA·Gal-T1 and Glc from the crystal structure suggested an explanation for the way in which LA modulates the acceptor specificity (10). The structural studies of the LA·Gal-T1 complex with UDP-Glc, together with the kinetic studies of Glc transfer from UDP-Glc to an acceptor sugar, also offered an explanation for the way in which LA modulates the donor specificity of Gal-T1 (7). In our continuing efforts to understand the structure and function of Gal-T1, we examined in the present study the interaction of UDP-GalNAc with Gal-T1. The results suggest that the formation of a hydrogen bond between GalNAc and Tyr-289 is responsible for the poor GalNAc-transferase activity that Gal-T1 exhibits. On the other hand, mutation of Tyr-289 to leucine, isoleucine, or asparagine enhances the GalNAc-transferase activity. Among these mutants, Y289L has GalNAc-transferase activity that is nearly equal to Gal-T activity.

MATERIALS AND METHODS

Site-directed Mutagenesis—Site-directed mutagenesis was performed using the PCR method. Construction of the mutants was done using plasmid pEGT-d129 as the template; this contains a *Bam*HI/*Eco*RI fragment inserted into pET23a vector, coding for residues 130–402 of bovine Gal-T1 (11), and has a Cys-342 to Thr mutation.

The mutation primers corresponding to the upper DNA strand are: Y289L, 5′-CCTTACGTG***CAATTG***TTTGGAGGTGTCTCTGCTCTAAGTAAA-3′ and 5′-GACACCTCCAAA***CAATTG***CACGTAAGGTAGGCTAAA-3′; Y289I, 5′-CTACCTTACGTGC***AGATCT***TTGGAGGTGTCTCTGCTCTAAG-3′ and 5′-GACACCTCCAAA***GATCT***GCACGTAAGGTAGG-

* This work was supported by federal funds from the NCI, National Institutes of Health, under Contract NO1-CO-12400. The costs of publication of this article were defrayed in part by the payment of page charges. This article must therefore be hereby marked "*advertisement*" in accordance with 18 U.S.C. Section 1734 solely to indicate this fact.

The atomic coordinates and structure factors (code 1L7W) have been deposited in the Protein Data Bank, Research Collaboratory for Structural Bioinformatics, Rutgers University, New Brunswick, NJ (http://www.rcsb.org/).

¶ To whom correspondence should be addressed: Structural Glycobiology Section, LECB, CCR, NCI-Frederick, Bldg. 469, Rm. 221, Frederick, MD 21702. Tel.: 301-846-1934; Fax: 301-846-7149; E-mail: qasba@helix.nih.gov.

[1] The abbreviations used are: β4Gal-T1, β1,4-galactosyltransferase I; LA, α-lactalbumin; LS, lactose synthase; wt, wild-type; r.m.s., root mean square; LacdiNAc, di-*N*-acetyllactosediamine; GalNAc-T, *N*-acetylgalactosyltransferase.

CTAATCCAA-3′; Y286N, 5′-GGATTAGCCTAC*CATATG*TGCAG**AAT**TTTGGAGGTGTCTCT-3′ and 5′-AGAGACACCTCCAAA**ATT**CTGCA-*CATATG*GTAGGCTAAATCC-3′. The restriction sites are shown in italics and the mutation codon in bold letters. Typically, the entire Gal-T1 DNA was PCR-amplified as two fragments using the terminal cloning primers and two mutagenesis primers. The fragments were then cut with the restriction enzymes *Mfe*I, *Bgl*II, and *Nde*I for Y286L, Y286I, and Y286N mutants, respectively, and ligated. The full Gal-T1 DNA with the mutation was amplified from the ligation mixture using the cloning primers and then inserted into the pET23a vector. Mutants were screened for the incorporated mutations, based on alterations in the restriction enzyme digestion patterns, and then sequenced. The positive clones were transformed into B834(DE3)pLysS cells as described previously (7). The mutant proteins were expressed and purified according to the published method (7).

Gal-T and GalNAc-T Enzyme Assays—The protein concentrations were measured using the Bio-Rad protein assay kit, based on the method of Bradford and further verified on SDS gel. An *in vitro* assay procedure for Gal-T1 has been reported previously (7). The activities were measured using UDP-Gal or UDP-GalNAc as sugar nucleotide donors, and GlcNAc and Glc as the acceptor sugars. For the specific activity measurements, a 100-μl incubation mixture containing 50 mM β-benzyl-GlcNAc, 10 mM $MnCl_2$, 10 mM Tris-HCl, pH 8.0, 500 μM UDP-Gal or UDP-GalNAc, 20 ng of Gal-T1, and 0.5 μCi of [^{3}H]UDP-Gal or [^{3}H]UDP-GalNAc was used for each Gal-T or GalNAc-T reaction. The incubation was carried out at 37 °C for 10 min. The reaction was terminated by adding 200 μl of cold 50 mM EDTA, and the mixture was passed through a 0.5-ml bed volume column of AG1-X8 cation resin (Bio-Rad) to remove any unreacted [^{3}H]UDP-Gal or [^{3}H]UDP-GalNAc. The column was washed successively with 300, 400, and 500 μl of water, and the column flow-through was diluted with Biosafe scintillation fluid; radioactivity was measured with a Beckman counter. A reaction without the acceptor sugar was used as a control. A similar assay was carried out to measure the GalNAc-T activity with Glc and other acceptors in the presence of 50 μM bovine LA (Sigma).

Studies for Determining the Kinetic Constants—The true K_m of the donor (K_A) and of the acceptor (K_B), the dissociation constant of the donor, $K_{i(a)}$, and k_{cat}, were obtained using two-substrate analyses and the primary plots of five concentrations of donor (UDP-Gal or UDP-GalNAc) and five concentrations of acceptor, and the corresponding secondary plots of the intercepts and slopes. Initial rate conditions were linear with respect to time. A suitable range of donor and acceptor concentrations were chosen, which allowed an accurate Michaelis-Menten plot to be derived. The data were also analyzed for a general two-substrate system using the following equations (12) with the software EnzFitter, a Biosoft nonlinear curve-fitting program for Windows.

$$v = \frac{V_{max}[A][B]}{K_{i(a)}K_B + K_B[A] + K_A[B] + [A][B]} \quad \text{(Eq. 1)}$$

$$v = \frac{V_{max}[A][B]}{K_B[A] + K_A[B] + [A][B]} \quad \text{(Eq. 2)}$$

Here v is the initial velocity and the rate equation for sequential symmetrical initial velocity pattern associated with Equation 1, an ordered or random equilibrium mechanism in which substrate A dissociates well from the E·S complex with a dissociation constant of $K_{i(a)}$. Equation 2 is for asymmetric initial velocity pattern for a double-displacement or "ping-pong" mechanism. The kinetic parameters K_A, K_B, $K_{i(a)}$, and V_{max}, were obtained from the fitted curves using the above rate equations. The graphical method and EnzFitter program gave very similar kinetic parameters. In the GalNAc-T assay, the maximum substrate concentrations used for UDP-GalNAc and GlcNAc were 1 and 200 mM, respectively. However, in the Gal-T assay, because of the limited solubility of GlcNAc in water, the concentration of GlcNAc was limited to no more than 400 mM (which is 2-fold higher than its K_m value), whereas up to 300 μM UDP-Gal were used.

^{1}H NMR Spectroscopy of the Product of GalNAc-T Activity—The reaction was carried out in a total volume of 1 ml that contained 100 μg of Y289L mutant plus 10 mM each triethanolamine-HCl, pH 8.0, UDP-GalNAc, GlcNAc, and $MnCl_2$ at 37 °C for 48 h. The mixture was first passed through a 1-ml Chelex 100 column and then through a 1-ml cationic column containing AG1-X8 resin (200–400-mesh). The disaccharide product in the flow-through from 4 bed volumes was pooled and freeze-dried. The product was finally dissolved in 400 μl of D_2O, and its ^{1}H NMR spectrum was obtained in a 400-MHz NMR spectrometer.

Crystal Structure Determination—The catalytic domain of the recombinant bovine Gal-T1 from residues 130 to 402 (mass ~33 kDa) and mouse recombinant LA (mass ~14 kDa) was co-crystallized in the presence of UDP-GalNAc and $MnCl_2$. The crystals were grown at room temperature by the hanging drop method, using 20 mg ml^{-1} Gal-T1 and 10 mg ml^{-1} LA in the presence of a substrate with the precipitant containing 100 mM NaCl, 100 mM sodium citrate buffer, pH 5.6, and 12.5% polyethylene glycol 4000. The crystals of the complex could only be obtained in the presence of 17 mM UDP-GalNAc and $MnCl_2$. Complete three-dimensional x-ray diffraction data were collected at beam line X9B, National Synchroton light source, Brookhaven National Laboratory, using a Quantum-4 ccd detector with 1.02-Å wavelength. The frames were processed using DENZO (13). The crystals belong to monoclinic, space group $P2_1$ with the cell constants a = 57.5, b = 95.7, c = 100.6 Å, and β = 101.4°. A total of 120,498 reflections were collected, of which 62,285 are unique (90% completeness), with an R_{sym} of 6.0%.

The crystal structures were solved by the molecular replacement method, using AMORE (14). The crystal structure of lactose synthase (9) without the substrate was used as the model for molecular replacement. After initial refinement, the difference electron density maps revealed the UDP-GalNAc and a Mn^{2+} ion bound to the Gal-T1 molecule and were included for further refinement. The two LS molecules in the asymmetric unit are related by a pseudo 2-fold symmetry. All the refinements were carried out initially by XPLOR3.85, followed by CNS1.0 (15). Only reflections with $F > 2\sigma(F)$ were used for the refinement. The final R factor for the 55,765 reflections is 23.2% with R_{free} (10% reflections) is 27%. The mean r.m.s. deviations of the bond lengths and angles are 0.001 Å and 0.01°, respectively. All the figures were drawn using MOLSCRIPT (16).

RESULTS AND DISCUSSION

Crystal Structure of Gal-T1·LA·UDP-GalNAc Complex and Molecular Interactions of UDP-GalNAc Molecule—The overall molecular structure and the interactions between Gal-T1 and LA molecules in the Gal-T1·LA·UDP-GalNAc·Mn^{2+} are quite similar to those observed in the previous crystal structure of Gal-T1·LA·UDP· Mn^{2+} complex (10). The mean r.m.s. deviation on Cα atoms between these two structures is only 0.7 Å (Fig. 1*A*), indicating that binding of UDP-GalNAc has neither perturbed the crystal structure of Gal-T1 nor its interactions with LA. In the crystal structure the UDP-GalNAc molecule and a Mn^{2+} ion could be clearly located from the electron density maps. The Mn^{2+} ion exhibits six coordinations: two with UDP-GalNAc, three with Gal-T1, and one with a water molecule (Table I). Although these coordinations are quite similar to those found in the previous crystal structure of the Gal-T1·LA·sugar nucleotide·metal complexes (7, 10), the sixth coordination with a water molecule has not been observed. Even though there is enough space available for this water molecule to coordinate with the Mn^{2+} ion in the previous crystal structures, none was observed (7, 10, 17). This may be because of the presence of the bulky *N*-acetyl group in UDP-GalNAc, which may better trap the water molecule.

Although the interactions of Gal-T1 with the GalNAc moiety of UDP-GalNAc are similar to the interactions of the Gal moiety of UDP-Gal (17), additional interactions are observed between the *N*-acetyl group of UDP-GalNAc with Gal-T1 (Fig. 1*B*). In the Gal-T1·UDP-Gal complex, the O2 hydroxyl group forms only one hydrogen bond with Asp-252, but in the present crystal structure the N2 nitrogen atom is hydrogen-bonded to the Asp-252 side chain carboxylate oxygen atom, whereas the carbonyl oxygen atom is hydrogen-bonded to the Tyr-289 side chain hydroxyl group. The presence of the *N*-acetyl group seems to have perturbed the conformation of both the GalNAc and the Tyr-286 side chain. The orientation of the *N*-acetyl group with respect to the sugar ring is represented by the torsion angle H2-C2-N2-HN, which in the case of GalNAc, GlcNAc, and ManNAc was observed to be nearly 180 ° (18). In the present crystal structure, there are two Gal-T1·LA·UDP-GalNAc·Mn^{2+} molecules in the asymmetric unit; in one molecule the torsion angle is 150° and in the other it is 120°, suggesting the existence of the *N*-acetyl group in an unfavorable orientation. This unfavorable orientation is a result of the

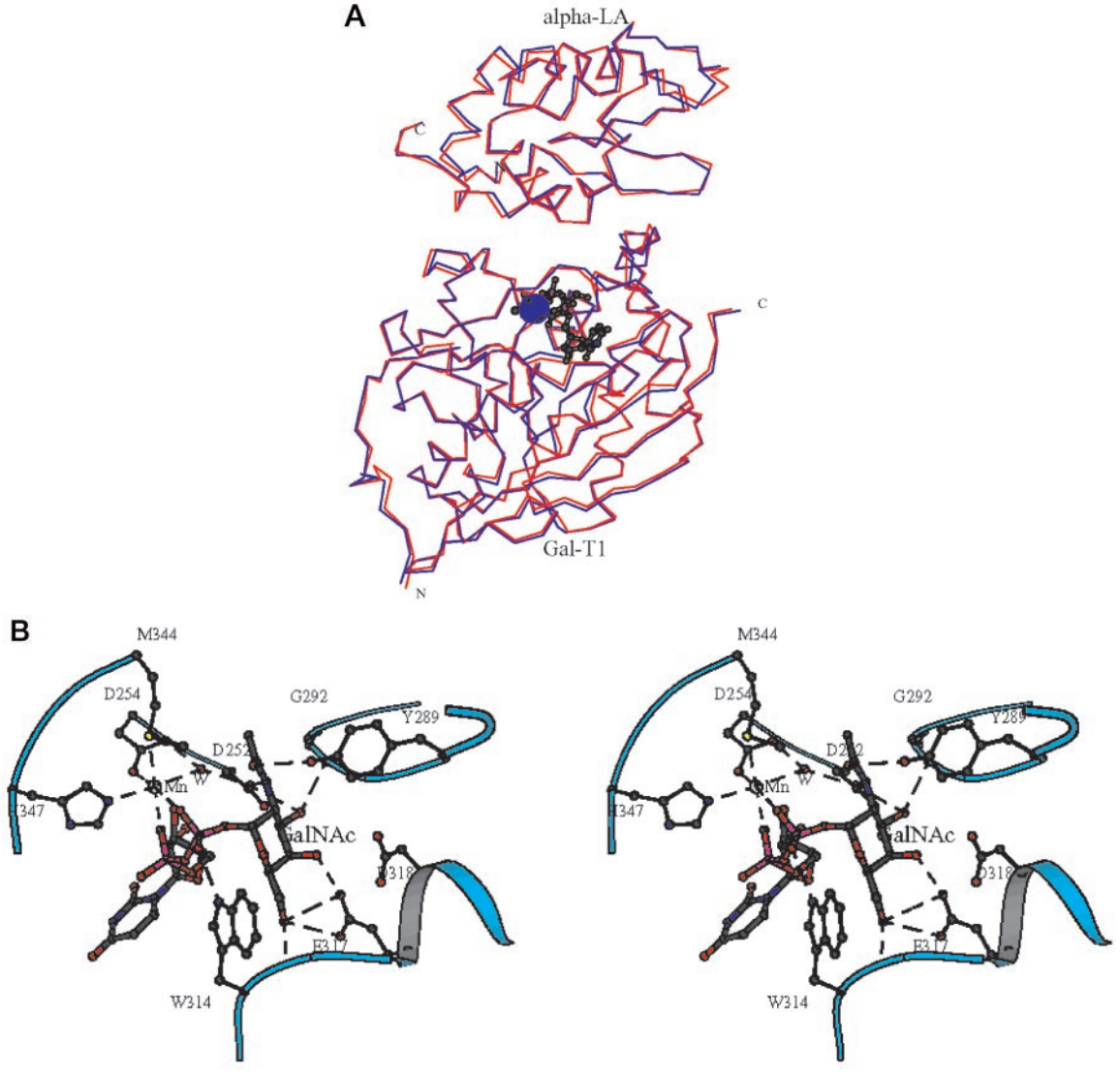

FIG. 1. *A*, superposition of the C atoms of the protein complex Gal-T1·LA·UDP-GalNAc·Mn^{2+} (*red*) with the Gal-T1·LA·UDP·Mn^{2+} complex (*blue*). The Mn^{2+} ion is shown as a *blue sphere* and UDP-GalNAc in *ball-and-stick*. The mean r.m.s. deviation between these two structures is only 0.7 Å, indicating that the overall structure of Gal-T1 and its interactions with LA have not been perturbed by the binding of UDP-GalNAc. The Protein Data Bank identification code for the coordinates of Gal-T1·LA·UDP-GalNAc·Mn^{2+} complex is 1L7W. *B*, molecular interactions between the GalNAc moiety of UDP-GalNAc and Gal-T1 molecule. The Mn^{2+} ion forms six coordinations; five are similar to the coordinations found in the crystal structure of Gal-T1·UDP-Gal·Mn^{2+} complex (17). The additional sixth coordination with a water molecule is only observed in the present crystal structure. Although the hydrogen bonding interactions observed are similar to that of Gal moiety with Gal-T1 in the Gal-T1·UDP-Gal complex, an additional hydrogen bond is observed between the carbonyl oxygen atom of the *N*-acetyl group of UDP-GalNAc and the side chain hydroxyl group of Tyr-289. This hydrogen bond seems to be hindering the GalNAc-transferase activity (see Fig. 2*B*). Additionally, the *N*-acetyl group seems to be in a less favorable orientation; the torsion angle H2-C2-N-HN being 120°, instead of 180° as is observed normally. All the hydrogen bonds are shown by *dashed lines*.

lack of space between the side chain hydroxyl group of Tyr-289 and the carbonyl oxygen atom of the *N*-acetyl group. In the two molecules of the asymmetric unit, because of this slight difference in the torsion angle of H2-C2-N2-HN, orientation of the side chain of Tyr-289 is slightly different to accommodate the *N*-acetyl group.

Effect of the N-Acetyl Group of GalNAc on GalNAc-T Activity—Among the interactions of the *N*-acetyl group of UDP-GalNAc with the Gal-T1 molecule, the hydrogen bond between the carbonyl oxygen atom of the *N*-acetyl group and the Tyr-289 side chain hydroxyl group seems to cause steric hindrance for catalysis. Studies using positional isotope exchange, secondary deuterium isotope effects, and inhibition of catalytic activity by acceptor analogs have suggested a plausible catalytic mechanism for the Gal-T1 (19–21). According to this mechanism, upon a nucleophilic attack from the O4 hydroxyl group of the acceptor molecule, Gal moiety, during its separation from UDP-Gal in the transition state complex, exits with a substantial sp^2 character at the anomeric center C1. Such an oxocarbonium ion intermediate forms a covalent linkage with the O4 oxygen atom, forming a β1–4 glycosidic linkage between galactose and the acceptor molecule. Because it is not feasible to obtain the crystal structure of Gal-T1 in the presence of both donor and acceptor molecules to determine the nature of interactions between the substrates and Gal-T1, we have carried out modeling studies based on the individual donor and acceptor bound to Gal-T1 structures (10, 17). These studies indicated that the O4 hydroxyl group of the acceptor lines up against the anomeric center C1 of the bound UDP-Gal molecule at 4.5 Å (Fig. 2*A*). During catalysis, this assembly of the substrates in the catalytic pocket requires the displacement of the substrates toward each other. Because any displacement of the acceptor GlcNAc toward the donor is prevented by Trp-314, it is most likely that the donor Gal moiety moves toward the acceptor

TABLE I
Mn^{2+} ion coordination distances in the crystal structure of Gal-T1·LA·UDP-GalNAc·Mn^{2+}

Unlike the earlier crystal structures (7, 9, 16), the present crystal structure shows the Mn^{2+} ion forming a sixth coordination with a water molecule (located only at 3σ).

Residue	Atom	Distance in molecule-1	Distance in molecule-2
		Å	Å
His-347	Nε2	2.43	2.29
UDP-GalNAc	O(Pα)	2.24	2.17
UDP-GalNAc	O(Pβ)	2.31	2.25
Met-344	Sδ	2.84	2.82
Asp-252	Oδ2	2.22	2.36
Water	O	2.57	2.35

during catalysis. In the Gal-T reaction, when the Gal moiety is involved during catalysis, there is enough space between the C2 atom of Gal and the side chain of Tyr-289, as the O2 hydroxyl group of Gal is facing away from the Tyr-289 residue (Fig. 2*A*). However, in the crystal structure of Gal-T1·LA·UDP-GalNAc·Mn^{2+}, the bulky *N*-acetyl group of GalNAc occupies this space with its carbonyl oxygen atom hydrogen-bonded to the hydroxyl group of Tyr-289 (Fig. 2*B*). We hypothesized from this observation that, during catalysis, this hydrogen bond is expected to hinder the reaction by not allowing the GalNAc moiety to move toward the acceptor molecule. Second, because of lack of available space between the *N*-acetyl group and Tyr-289, the former exists in a less favorable orientation. To create the space in the Gal-T1 molecule in the vicinity of the *N*-acetyl group binding site of UDP-GalNAc, we mutated the Tyr-289 residue to Leu, Ile, or Asn (Fig. 2*C*). A phenylalanine mutation was not considered, because it does not create enough space when the *N*-acetyl group adopts its favorable conformation. Although Leu or Asn residue substitution creates a similar pocket because of the similarity of their side chain length (Fig. 2*C*), Leu is expected to create a hydrophobic pocket whereas Asn creates a hydrophilic one. Additionally, because of its shorter side chain length, an Ile substitution would be expected to create even a larger pocket size than the Leu substitution. Thus, investigations of these three mutants were expected to identify the required size and the nature of the pocket in the vicinity of the *N*-acetyl group-binding site of UDP-GalNAc.

Comparison of Gal-T and GalNAc-T Catalytic Activities of Wild-type and Gal-T1 Mutants—The mutants Y289L, Y289N, and Y289I exhibit both Gal-T and GalNAc-T activities at the saturation substrate concentrations (Table II and Fig. 3). The mutants Y289L and Y289N exhibit equally strong Gal-T and GalNAc-T activities, suggesting that a Leu or Asn substitution of Tyr-289 seems to create the required optimal space. The specific GalNAc-T activity of the mutant Y289I at the saturation concentration is half that of Y289L (Table II); it exhibits a slightly weaker affinity to UDP-GalNAc (Fig. 3). Therefore, an Ile substitution seems to create more than the required space, thus reducing the specific activities. Although Asn substitution exhibits the GalNAc-T activity as well as the Leu substitution, the protein seems to be less stable and tends to denature rapidly compared with the Leu mutant. It has been shown that wt-Gal-T1 exhibits a very low glucosyltransferase activity (Glc-T), but no *N*-acetylglucosaminyltransferase (GlcNAc-T) activity (3, 6, 7). On the contrary, the mutants exhibit reasonable GlcNAc-T activity (Table II) where they transfer GlcNAc from UDP-GlcNAc to the acceptor GlcNAc but do not exhibit Glc-T activity. It is interesting to note that in this GlcNAc-T activity the initial product, the disaccharide GlcNAc β1,4-GlcNAc, itself is an acceptor for the enzyme, thus producing tri- and longer

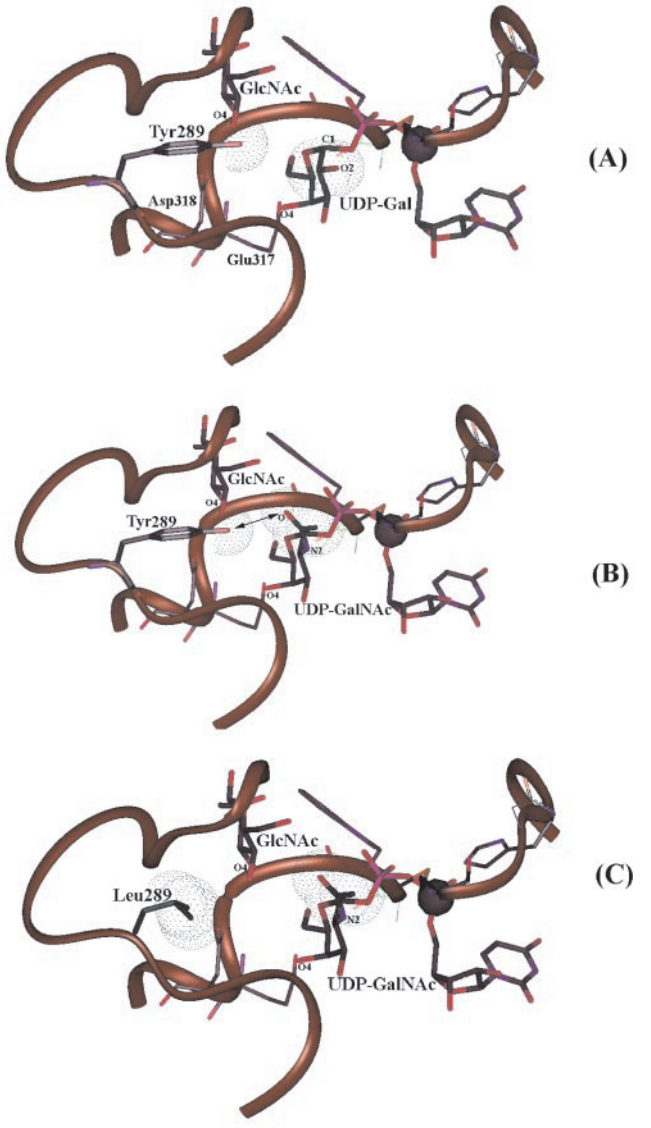

FIG. 2. *A*, modeling of the GlcNAc in its binding site (based on the crystal structure of Gal-T1·LA·GlcNAc complex) on the Gal-T·UDP-Gal·Mn^{2+} crystal structure (17). As can be seen, the acceptor atom O4 of GlcNAc is in the proper orientation with the anomeric center (C1 atom) of the Gal moiety of UDP-Gal. The distance between these atoms is ~4 Å. It has been hypothesized that the enzyme catalysis follows the separation principle, in which the Gal moiety is expected to move toward the acceptor while forming the disaccharide. Because there is enough space between Tyr-289 and the Gal moiety, Tyr-289 is not expected to hinder the Gal-T activity. This is illustrated by the *dotted surface* showing the van der Waals sphere for the Tyr-289 side chain hydroxyl group and the C2 and O2 atoms of the Gal moiety. *B*, modeling of the GlcNAc in its binding site on the Gal-T1·LA·UDP-GalNAc·Mn^{2+} crystal structure. Because LA does not interact with the donor molecule, it is not shown in the figure. Similar to UDP-Gal binding (Fig. 2*A*), the O4 atom of GlcNAc is located ~4 Å away from the anomeric center of GalNAc moiety of UDP-GalNAc. The major difference between the binding of UDP-Gal and UDP-GalNAc seems to be an additional hydrogen bond observed between the *N*-acetyl group and Gal-T1, particularly with Tyr-289. The side chain hydroxyl group of Tyr-289 is hydrogen-bonded with the carbonyl oxygen atom of the *N*-acetyl group of GalNAc (shown by *double arrow*). If the catalytic mechanism still follows the separation principle, this hydrogen bond would hinder the required displacement of the GalNAc moiety during the disaccharide linkage formation. As can be seen from the van der Waals sphere (*dotted surface*), little space exists between the Tyr side chain hydroxyl group and the *N*-acetyl group. Therefore, based on this observation, it was hypothesized that lack of space is responsible for the poor GalNAc-T activity. *C*, based on the hypothesis that more space is needed between the *N*-acetyl group of UDP-GalNAc and Tyr-289 residue to facilitate the reaction, the substitution of Tyr-289 by Leu is modeled. The van der Waals sphere shown in *dotted surface* for the side chain atoms of Leu-289 and the *N*-acetyl group clearly indicates that such substitution creates additional space.

TABLE II

Specific activities of the catalytic domain of Gal-T1 (d129-Gal-T1, residues 130–402) with C342T mutation and the Tyr-289 mutants

Reactions were performed under saturating conditions of all substrates (see "Materials and Methods" for assay conditions). In these reactions, the concentration for the donors was at 500 μM and the acceptor β-benzyl-GlcNAc was at 25 mM. In the Gal-T reaction of C342T, the acceptor concentration was 10 mM, because at 25 mM it showed inhibition. Because Y289N rapidly undergoes denaturization, reliable data could not be obtained.

Enzyme	UDP-galactose → GlcNAc Gal-T activity	UDP-GalNAc → GlcNAc GalNAc-T activity	UDP-GlcNAc → GlcNAc GlcNAc-T activity
	pmol/min/ng	*pmol/min/ng*	*pmol/min/ng*
C342T	11.8	0.1	0
Y289L_C342T	16.2	27.3	8.2
Y289I_C342T	3.8	14.7	6.2

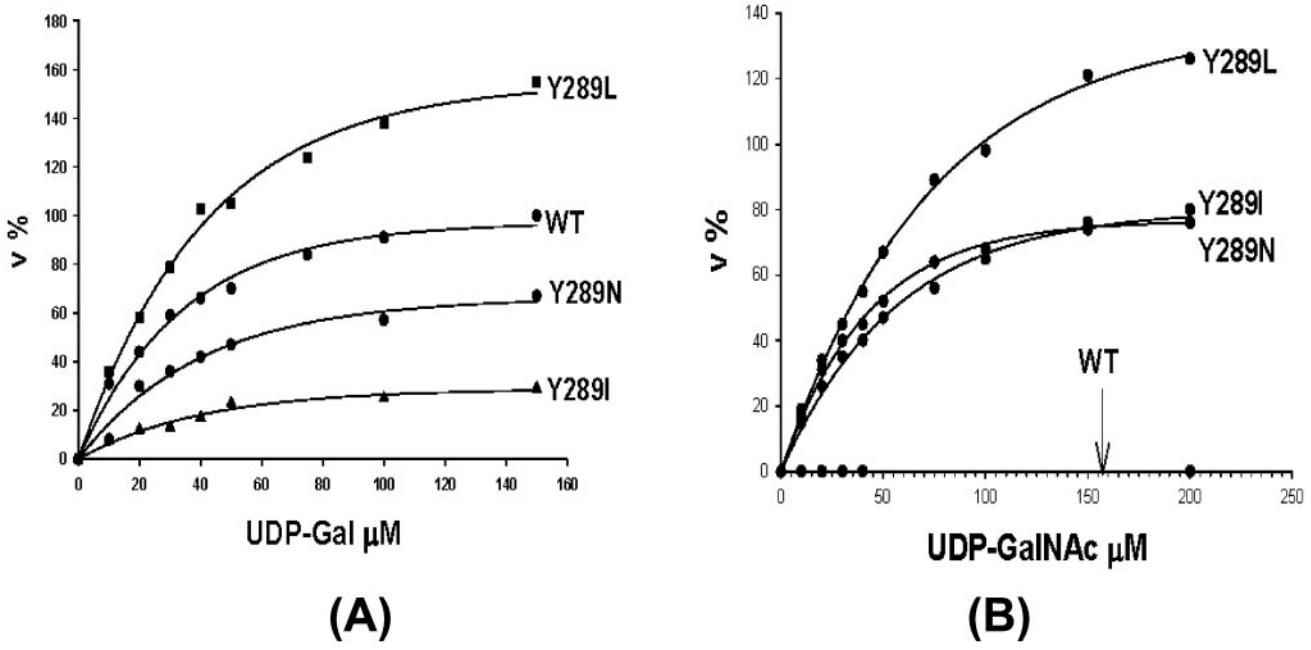

FIG. 3. **The catalytic activity of the wt-Gal-T1 and the mutantsY289L, Y289I, and Y289N.** *A*, Gal-T activity of wt-Gal-T1 and of mutants at the saturating concentrations of β-benzyl-GlcNAc as the acceptor (see "Materials and Methods"). The mutant Y289L seems to be as active as the wt-Gal-T1, whereas Y289I seems to be weaker. *B*, GalNAc-T activity of the wt-Gal-T1 and of mutants. The wt-Gal-T1 exhibits very poor GalNAc-T activity, whereas Y289L exhibits more GalNAc-T activity than its Gal-T activity. Y289I exhibits a somewhat weaker GalNAc-T activity, compared with that of Y289L. The activities are measured with 50 mM β-benzyl-GlcNAc as acceptors at different concentrations of the donor. The Gal-T activity of the wt-Gal-T1 was measured with only 10 mM β-benzyl-GlcNAc, because it showed inhibitions at 50 mM concentration.

TABLE III

Kinetic parameters for the donor and the acceptor substrates by Y289L_C342T mutant in the Gal-T and GalNAc-T catalytic reactions (see text for assay conditions)

ND, not determined.

Mutant	Gal-T UDP-galactose → GlcNAc			GalNAc-T UDP-*N*-acetylgalactosamine → GlcNAc		
	K_A	K_B	k_{cat}	K_A	K_B	k_{cat}
	μM	mM	s^{-1}	μM	mM	s^{-1}
C342T	93 (6)	11 (1)	14	ND	ND	ND
Y289L_C342T	75 (1)	198 (1)	8.5	354 (3)	51 (1)	40

chain saccharides. A separate study on this GlcNAc-T property is being carried out.

Because the Y289L variant of Gal-T1 exhibits both Gal-T and GalNAc-T enzyme activities with equal efficiencies, double substrate kinetic studies were carried out to determine the kinetic constants for both the donor and acceptor molecules. The kinetic data from both reactions fit best to Equation 2, with a zero $K_{i(a)}$ value, describing an asymmetric initial velocity pattern for a double-displacement or "ping-pong" mechanism. The Y289L mutant in the Gal-T reaction shows for the acceptor nearly 20-fold higher K_m than the wild-type Gal-T1 (Table III). The catalytic constant (k_{cat}) in the Gal-T1 reaction is comparable with the wild type, but it is nearly 3–5-fold higher in the GalNAc-T reaction (Table III). It is possible that this high k_{cat} was achieved either by stabilizing the transition state or by the increase in the free energy of the ternary complex. Although the mutation was designed to eliminate the steric hindrance caused by Tyr-289 during the transition state, the latter possibility cannot be ruled out because of the observed high K_m value for the acceptor GlcNAc. In the crystal structure of Gal-T1, the residues around Tyr-289 are involved in the acceptor binding. The lack of an aromatic side chain at position 289 may destabilize these residues, thus affecting the binding of the acceptor substrate. This is substantiated by the earlier mutational studies on human Gal-T1, where substitution by Phe for the corresponding residue Tyr-287 does not affect the acceptor binding, whereas substitution with Gly totally abolished the catalytic activity (22). Currently, mutational studies are being

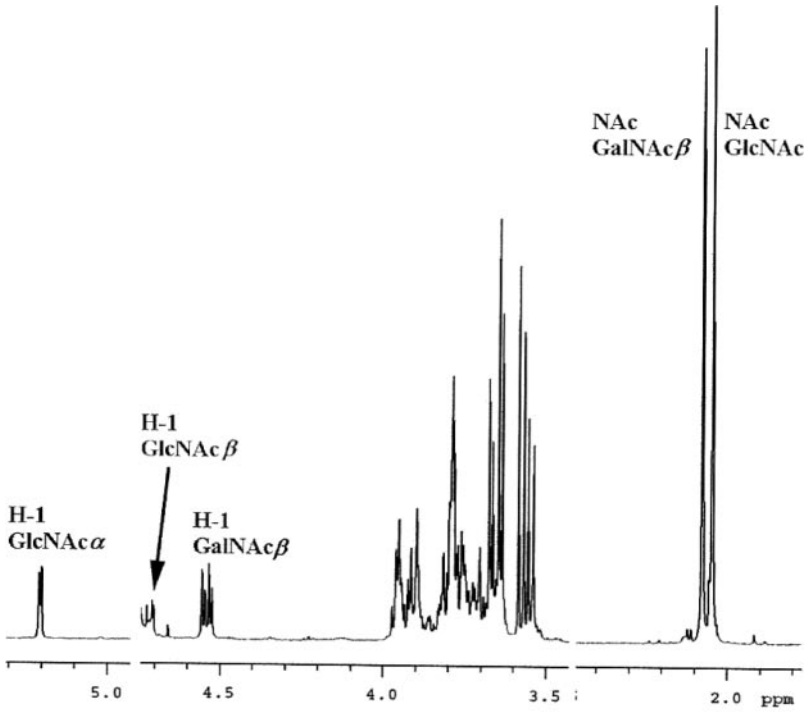

FIG. 4. **Partial ^{1}H NMR spectrum of the disaccharide (LacdiNAc) product from the GalNAc-T reaction with GlcNAc as the acceptor.** The NMR spectrum is quite similar to that of the LacdiNAc product obtained using bovine mammary gland β1,4-*N*-acetylgalactosaminyltransferase (25). The signal for the GalNAc anomeric proton is at δ 4.53 ppm and for the GlcNAc anomeric proton corresponding to an α and a β conformer is at δ 5.2 and 4.7 ppm. The signals from the acetyl group of each sugar moiety are at δ 2.05 and 2.08 ppm.

carried out to enhance the acceptor affinity of Y289L mutant to determine which mechanism is responsible for the high catalytic efficiency of the enzyme.

Although the weak GalNAc-T activity of the wild-type Gal-T1 had been demonstrated in the earlier studies and the product disaccharide, di-*N*-acetyllactosediamine (LacdiNAc), was characterized by ^{1}H NMR technique, no details were reported (6). Because the Y289L mutant exhibits equally high GalNAc-T activity as it does Gal-T activity, the disaccharide product from this reaction was purified and analyzed by ^{1}H NMR spectroscopy (Fig. 4). Previously, the same product LacdiNAc, from a *N*-acetylgalactosaminyltransferase isolated from bovine mammary gland, had been fully characterized by ^{1}H NMR spectroscopy (23). The present NMR spectrum is quite similar to that of the already characterized LacdiNAc, demonstrating that the mutant Y289L transfers GalNAc from UDP-GalNAc to GlcNAc, forming a β1–4 linkage between GalNAc and GlcNAc.

A Point Mutation in the Codon for Amino Acid 289 Can Convert the Enzyme with Dual Property—In humans, the β4Gal-T family has seven members (Gal-T1 to -T7), each with high sequence identity within their catalytic domain (24, 25). These family members are known to transfer Gal from UDP-Gal to different sugar acceptors. For example, Gal-T6 transfers Gal to Glc of Glc-ceramide, whereas Gal-T7 transfers Gal to xylose (25). Among these seven members, four members, Gal-T1 to Gal-T4, have a Tyr residue at position 287 (which corresponds to Tyr-289 in bovine Gal-T1), whereas Gal-T5 and Gal-T6 have a Phe residue. Mutational studies in human Gal-T1 have shown that theY287F mutant exhibits the same enzyme characteristics with kinetic constants as that of the wild-type Gal-T1 (22). Because the Phe residue may also create a similar steric problem for UDP-GalNAc as the Tyr residue, these enzymes are expected to exhibit low GalNAc-T activity. It is interesting to note that the family members show variation in their codon nucleotide sequence for residue 287 (Table IV), particularly at the second and third nucleotide positions of the codon. A mutation of the first nucleotide base thymidine (T) to either adenine (A) or cytidine (C) would result in a mutation of the Tyr/Phe residue to either Leu or Asn. Such a spontaneous point mutation at the first nucleotide position of the codon for the residue 287 would generate an enhanced equal GalNAc-transferase activity that might have adverse effects. Incorporation of GalNAc instead of Gal might lead to 1) termination of the total synthesis of a glycoconjugate, or 2) glycans with different oligosaccharide sequence. It is worth noting, however, that, although mutants may possess dual enzyme activities, the substitution of Gal by GalNAc is expected to be highly

TABLE IV
Codon usage for the amino acid at position 289 among the Gal-T1 family members

In human Gal-T1 the corresponding amino acid is at position 287. The second and third nucleotides of the codon show variations among the family members, while strictly conserving the first nucleotide. Mutation of the first nucleotide of the codon (shown in bold) to either A or C would result in a Leu or Asn residue instead of Tyr, and such mutant would exhibit dual enzymatic activities.

Enzyme	Codon	Amino acid at position 289
Bovine Gal-T1	**T**AT	Tyr
Human Gal-T1	**T**AT	Tyr
Human Gal-T2	**T**AC	Tyr
Human Gal-T3	**T**AC	Tyr
Human Gal-T4	**T**AT	Tyr
Human Gal-T5	**T**TT	Phe
Human Gal-T6	**T**TC	Phe
Human Gal-T7	**T**AC	Tyr

TABLE V
GalNAc-T catalytic activity of Y289L mutant in the absence and the presence of LA on various acceptor substrates

Assays were carried out at 37 °C using 500 μM UDP-GalNAc for 10 minutes. In all the measurements, the acceptor concentration was 100 mM and the LA concentration was 55 μM.

Acceptor	GalNAc-T activity	
	−LA	+LA
	pmol/min/ng	
GlcNAc	31.3	3.3
Glc	2.6	34.8
Glucosamine	1.8	5.0

irregular and will depend on whether or not UDP-GalNAc is available in the Golgi apparatus.

Role of LA in the GalNAc-T Activity of the wt-Gal-T1 and the Y289L Mutant—Although Gal-T1 transfers GalNAc from UDP-GalNAc to GlcNAc with ~0.1% of its Gal-T efficiency, it has been shown that LA enhances this transfer (5), a situation similar to glucosyltransferase activity (Glc-T) of Gal-T1, where LA increases this activity from 0.3 to 10% (7). We have shown previously through crystal structure and enzyme kinetic studies that, in the Glc-T reaction, LA plays a kinetics role in stimulating Gal-T1 to transfer Glc from the UDP-Glc to GlcNAc (7, 9). Although we have not carried out detailed kinetic studies on the GalNAc-T reaction by the wild-type Gal-T1 in the presence of LA, the similarity between Glc-T and GalNAc-T catalytic activities indicates that LA probably plays a similar role in the GalNAc-T reaction. It has been stated that LA enhances this GalNAc-T activity to 55% of its Gal-T activity (5); however, we find that the activity is enhanced only to nearly 1% (data not shown). This may have been because of the differences in the assay methods. For example, in the present study and the studies reported by others (12), the donor concentration is determined by the unlabeled UDP-sugar, and only a small amount of ^{3}H-labeled UDP-sugar is used during the assay. Therefore, the catalytic activity is determined accurately by the amount of unlabeled UDP-sugar used, whereas, in the previous study (5), the specific activity of the ^{3}H-labeled UDP-GalNAc provided by the manufacturer was used to determine the specific activity of the enzyme.

Unlike wt-Gal-T1, where LA stimulates the transfer of GalNAc only to GlcNAc and not to Glc (5), the Tyr-289 mutants (Y289L, Y289N, and Y289I) in the presence of LA transfer GalNAc preferably to Glc rather than to GlcNAc. This property is quite similar to LS activity in which the wt-Gal-T1 in the presence of LA transfers Gal to Glc instead to GlcNAc (Table V). Furthermore, like wt-Gal-T1, these mutants also transfer Gal to Glc in the presence of LA (data not shown). For example, an *N*-acetylgalactosaminyltransferase activity in the bovine mammary gland extracts with a similar catalytic property has been identified (26). This enzyme also transfers GalNAc from UDP-GalNAc to GlcNAc in the absence of LA, whereas in the presence of LA it transfers GalNAc to Glc instead to GlcNAc. In fact, a small amount of the lactose analogue GalNAcβ1–4Glc is found in the milk (26). However, the protein sequence for this *N*-acetylgalactosaminyltransferase is not yet known. Thus, it seems that an *N*-acetylgalactosaminyltransferase enzyme is present in cells with enzyme properties similar to the present mutants. The exact nature and the function of the oligosaccharide synthesized involving this enzyme are not yet known. It has been pointed out that, in Madin-Darby canine kidney cells, large amounts of *N*-glycans are found to carry GalNAc instead of Gal, linked β1,4 to GlcNAc (27).

Conclusion—The crystal structure of UDP-GalNAc bound to Gal-T1 shows that the carbonyl oxygen atom of the *N*-acetyl group of GalNAc is hydrogen-bonded to the hydroxyl group of Tyr-289, which hinders the transfer of GalNAc during catalysis. For the Gal-T1 to function efficiently as GalNAc-T, an optimal space for the binding of the *N*-acetyl group of UDP-GalNAc to Gal-T1 is required, and such a space need not be hydrophobic nor hydrophilic in nature. In the present study, we have shown that the Tyr-289 mutants of Gal-T1, which have an optimal space for the binding of *N*-acetyl group, exhibit as high GalNAc-T activity as Gal-T activity, as well as GlcNAc-T activity. In the human Gal-T family members, the Tyr/Phe residue at 287 (or in bovine Tyr-289) seems to be important for determining the donor sugar specificity of these enzymes, and mutation of this residue broadens the donor specificity of the enzyme. The present study suggests that a single point mutation can result in glycan moieties substituting Gal with GalNAc or GlcNAc, which may have significant effects on cellular functions.

Acknowledgments—We thank Dr. Zbgniew Dauter for help with synchrotron data collection. We thank Dr. Soma Kumar for helpful discussions and comments during preparation of the manuscript. All the NMR spectra were recorded in the Analytical Chemistry Laboratory, NCI-Frederick (Frederick, MD). The primers were synthesized by the Molecular Technology Laboratory, NCI-Frederick.

REFERENCES

1. Hill, R. (1979) *UCLA Forum Med. Sci.* **21,** 63–86
2. Berliner, L. J., Davis, M. E., Ebner, K. E., Beyer, T. A., and Bell, J. E. (1984) *Mol. Cell. Biochem.* **62,** 37–42
3. Berliner, L. J., and Robinson, R. D. (1982) *Biochemistry* **21,** 6340–6343
4. Andree, P. J., and Berliner, L. J. (1978) *Biochim. Biophys. Acta* **544,** 489–495
5. Do, K. Y., Do, S. I., and Cummings, R. D. (1995) *J. Biol. Chem.* **270,** 18447–18451
6. Palcic, M. M., and Hindsgaul, O. (1991) *Glycobiology* **1,** 205–209
7. Ramakrishnan, B., Shah, P. S., and Qasba, P. K. (2001) *J. Biol. Chem.* **276,** 37665–37671
8. Qasba, P. K., and Kumar, S. (1997) *Crit. Rev. Biochem. Mol. Biol.* **32,** 255–306
9. Ramakrishnan, B., Boeggeman, E., and Qasba, P. K. (2002) *Biochem. Biophys. Res. Commun.* **291,** 1113–1118
10. Ramakrishnan, B., and Qasba, P. K. (2001) *J. Mol. Biol.* **310,** 205–218
11. Boeggeman, E. E., Balaji, P. V., Sethi, N., Masibay, A. S., and Qasba, P. K. (1993) *Protein Eng.* **6,** 779–785
12. Zhang, Y., Malinovskii, V. A., Fiedler, T. J., and Brew, K. (1999) *Glycobiology* **9,** 815–822
13. Otwinowski, Z., and Minor, W. (1997) *Methods Enzymol.* **276,** 307–326
14. Navaza, J. (1994) *Acta Crystallogr. Sect. A* **50,** 760–763
15. Brunger, A. T., *et al.* (1998) *Acta Crystallogr. Sect. D Biol. Crystallogr.* **54,** 905–921
16. Karulis, P. J. (1991) *J. Appl. Crystallogr.* **24,** 946–950
17. Ramakrishnan, B., Balaji, P. V., and Qasba, P. K. (2002) *J. Mol. Biol.* **318,** 491–502
18. Rao, V. S. R., Qasba, P. K., Balaji, P. V., and Chandrasekaran, R. (1998) *Conformation of Carbohydrates*, Harwood Academic Publishers, Amsterdam, Netherlands
19. Kim, S. C., Singh, A. N., and Raushel, F. M. (1988) *Arch. Biochem. Biophys.* **267,** 54–59
20. Hindsgaul, O., Kaur, K., Srivastava, G., Blaszczyk-Thurin, M., Crawley, S. C., Heerze, L. D., and Palcic, M. M. (1991) *J. Biol. Chem.* **266,** 17858–17862
21. Chung, S. J., Takayama, S., and Wong, C. H. (1998) *Bioorg. Med. Chem. Lett.* **8,** 3359–3364
22. Aoki, D., Appert, H. E., Johnson, D., Wong, S. S., and Fukuda, M. N. (1990) *EMBO J.* **9,** 3171–3178
23. Van den Nieuwenhof, I. M., Schiphorst, W. E., Van Die, I., and Van den Eijnden, D. H. (1999) *Glycobiology* **9,** 115–123
24. Lo, N. W., Shaper, J. H., Pevsner, J., and Shaper, N. L. (1998) *Glycobiology* **8,** 517–526
25. Nomura, T., Takizawa, M., Aoki, J., Arai, H., Inoue, K., Waskisaka, E., Yoshizuka, N., Imokawa, G., Dohmae, N., Takio, K., Hattori, M., and Matsuo, N. (1998) *J. Biol. Chem.* **273,** 13570–13577
26. Van den Nieuwenhof, I. M., Schiphorst, W. E., and Van den Eijnden, D. H. (1999) *FEBS Lett.* **459,** 377–380
27. Van den Nieuwenhof, I. M., Koistinen, H., Easton, R. L., Koistinen, R., Kamarainen, M., Morris, H. R., Van Die, I., Seppala, M., Dell, A., and Van den Eijnden, D. H. (2000) *Eur. J. Biochem.* **267,** 4753–4762